Supporting Information

A supramolecular strategy for the control of thermal expansion in molecular crystals

Masato Haneda, Kiyonori Takahashi,* Naohiro Hasuo, Rui-Kang Huang, Chen Xue, Jia-bing Wu, Shin-ichiro Noro, Seiji Tsuzuki, Sadafumi Nishihara and Takayoshi Nakamura*

E-mail: ktakahashi@kumamoto-u.ac.jp (K.Takahashi), tnakam@hiroshima-u.ac.jp (T.Nakamura)

General. All reagents purchased were used without further purification. Elemental analyses were carried out by using a CHN analyzer (CE440, Exeter Analytical, Inc.) at Global Facility Center , Hokkaido University.

Synthesis. Precursor of $(TBA^+)[Ni(dmit)_2]^-$ (TBA^+= tetra-*n*-butylammonium$^+$) and $(({}^+H_3N\text{-}C_2H_4)_2O)(BF_4^-)_2$ were prepared using a procedure reported in the literature.[28,50] A solution of $(TBA^+)[Ni(dmit)_2]^-$ (20 mg, 0.04 mmol) in CH_3CN (20 mL) was added to a solution of benzo[18]crown-6 (128 mg, 0.35 mmol) and $(({}^+H_3N\text{-}C_2H_4)_2O)(BF_4^-)_2$ (37 mg, 0.13 mmol) in CH_3CN (19 mL) and CH_3OH (1 mL). Crystal **1** was obtained by slow diffusion over a period of 4 days. Elemental analysis for crystal **1**: calcd. for $C_{48}H_{62}N_2Ni_2O_{13}S_{20}$: C: 33.31%, H: 4.00%, N: 1.77%, Found : C: 35.15%, H: 3.73%, N: 1.71%.

Crystal structure determination. Temperature-dependent structural analysis of the single crystal **1** was performed using a Rigaku XtaLAB-Synergy diffractometer with a HyPix-6000 area detector and multilayer mirror-monochromated Mo Kα radiation (λ = 0.71073 Å). A single crystal was mounted on a MicroMountsTM tip (MiTeGen) with Paratone 8277 (Hampton Research). The temperature dependence was measured using the same crystal. For the reflection data, multi-scan absorption corrections were applied to the crystals. Data collection was performed and processed using the CrysAlisPRO interface (Oxford Diffraction, Agilent Technologies UK Ltd). The initial structure was solved using SHELXT,[51] and structural refinement was performed using OLEX2 software.[52] Anisotropic refinement was applied to all atoms, except for the hydrogen atoms. CCDC 2444930-2444943 for crystal **1** at 110-320 K, respectively). The CLTE was calculated using the *PASCal* web program based on the unit cell parameters at each temperature.[29]

Physical Property Measurements. Differential scanning calorimetry (DSC) measurements were carried out using a Q2000 differential scanning calorimeter (TA Instruments) in the temperature range from 240 to 300 K at a scanning rate of 5 K min^{-1} under a flow of N_2 gas (50 mL min^{-1}). The temperature-dependent χ_m for polycrystalline sample of **1** was measured using a Quantum Design MPMS-3 SQUID magnetometer. Prior to sample measurement, the magnetic susceptibility of the sample holder (aluminum wrap) was measured under identical conditions, then the susceptibility of the holder was subtracted from the gram susceptibility as the paramagnetic contribution. The diamagnetic component in the sample was subtracted based on Pascal's constant, -4.2465×10^{-4} cm^3 mol^{-1}.[53] A magnetic field of 1 T was applied for all temperature-dependent measurements. Molecular weight of 816.805 g mol^{-1} (the χ_m for two $[Ni(dmit)_2]^-$ molecules) was used for calculation of χ_m of crystal **1**. Temperature- and frequency-

dependence of dielectric constant was measured using an impedance analyzer 4294A (Agilent) with the four-probe AC impedance method at a frequency range of $10^{2.5}$–10^{6} Hz. The temperature was controlled using cryostats with temperature controller models 331 (Lake Shore Cryotronics Inc.). Electrical contacts were prepared using a silver paste (D-500, Fujikura Kasei Co.,Ltd.) to attach the 25 μm ϕ gold wires to the pelletized sample.

Theoretical calculation. The extended Hückel molecular orbital method within the tight-binding approximation was applied to calculate the transfer integral (*t*) data between the $[Ni(dmit)_2]^-$ anions in crystal **1**. The lowest unoccupied molecular orbital of the $[Ni(dmit)_2]^-$ molecule was used as the basis function. According to the literature, semiempirical parameters for Slater-type atomic orbitals were obtained. The *t* values between each pair of molecules were assumed to be proportional to the overlap integral (*S*) according to the equation $t = -10S$ (eV).[47] The intermolecular interactions between **CE1•••CE1** and **CEA1•••CEA1** were estimated from computations at the B3LYP/6-31G(d,p) level.[54] Grimme's D3 dispersion model was used for dispersion correction.[42] Computations were performed using the GAUSSIAN16 code set.[55] To remove errors due to the overestimation of interaction energy (basis set superposition error), the counterpoise correction implemented in GAUSSIAN16 was applied.[56] The geometric parameters of in the calculation were used based on the hydrogen atom positions modeled in X-ray crystal structure analysis.[49,51]

§Table S1. Representative zero thermal expansion crystals of organic and inorganic crystals.

Materials Name	CLTE (α, $\times10^{-6}$ K^{-1})	References
$((^{+}H_3N–C_2H_4)_2O)(B[18]crown\text{-}6)_2([Ni(dmit)_2]^{-})_2$	−0.99 (110-190 K)	This study
IMD-OXA	+0.30 (100-400 K)	[8]
Al-TCPP-Ni	+0.31 (125-475 K)	[39]
$Eu_2(ox)(glc)_4$	+1.74 (105-250 K)	[42]
Zn-DMOF-TM x	−10 (~288 K)	[43]
(3-chloro-adamantane-1-ammonium)([18]crown-6)(ClO_4^{-})	−3.1 (250-317 K)	[27]
$Zn_4O(CO_2)_6$	−0.14 (300-600 K)	[44]
$Fe_{2.5}Hf$	+0.40 (433-583 K)	[57]
Ho_xFe_{1-x} (x = 0.04)	+0.19 (100~335 K)	[58]
glass ceramics	+1.0 (273-323 K)	[36]
$LaFe_{11.0}Si_{2.0}$	+0.50 (20-275 K)	[59]
$TbCo_{1.9}Fe_{0.1}$ (Rare-Earth-Based Alloy)	+0.48 (123-307 K)	[60]
$(1-x)PbTiO_3-xBi(Ni_{1/2}Ti_{1/2})O_3$ (x = 0.2)	+0.38 (25-525 K)	[61]
(Zr, Nb)Fe_2	+0.47 (4-425 K)	[62]
$NaZn_{13}$-type La(Fe,Si)$_{13}$	< +1.0 (15-150 K)	[63]
$K_6Cd_3(C_3N_3O_3)_4$	0.06 (10-130 K)	[64]
$Cs^{I}_{0.94}Mn^{II}[Fe^{II}(CN)_6]_{0.21}[Fe^{III}(CN)_6]_{0.70}\cdot0.8H_2O$	+0.20 (20-300 K)	[65]
PbC_4O_4	-0.61 (125-500 K)	[66]

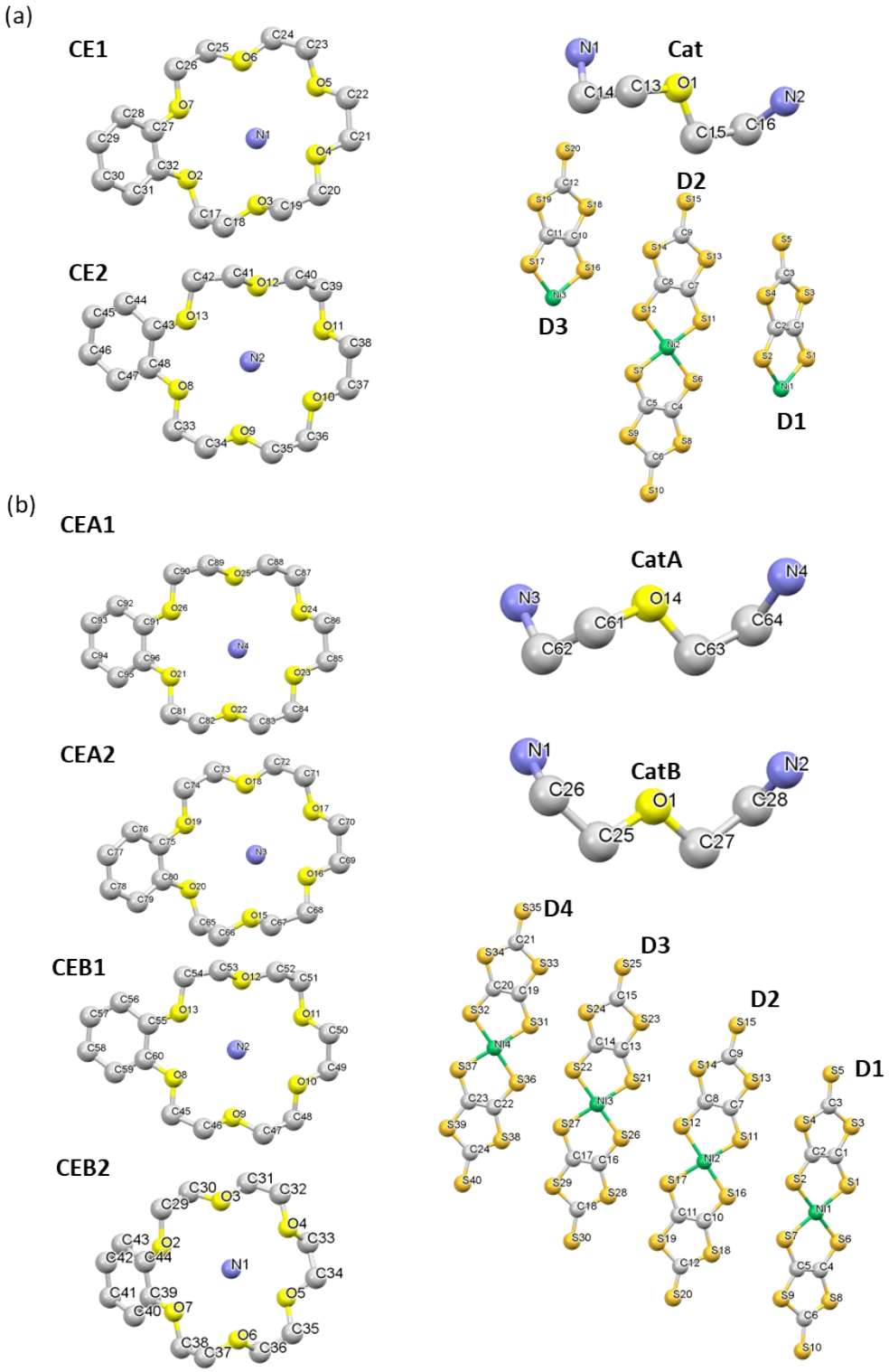

§Figure S1. Crystallographically independent structures of crystal **1** at 110 K (a) and 270 K (b). The Ni, S, C, N, and O atoms are depicted in green, orange, gray, blue, and yellow, respectively. All molecules are depicted as ellipsoid models. Hydrogen atoms are omitted for clarity.

§Table S2. Distances and angles for N-H•••O hydrogen bonding at 110 and 270 K

list of atoms	**N•••O distance** / Å	**H•••O distance** / Å	**N-H•••O angle** / °
110 K			
N1-H1A•••O3	2.744(2)	1.947	150.2
N1-H1B•••O7	3.014(2)	2.292	136.1
N1-H1C•••O5	2.927(2)	2.189	137.7
N2-H2A•••O12	2.886(2)	2.045	152.9
N2-H2B•••O10	2.899(2)	2.022	161.6
N2-H2C•••O8	2.924(2)	2.035	165.4
270 K			
N1-H1A•••O3	2.808(5)	1.966	157.2
N1-H1B•••O7	3.042(5)	2.408	128.4
N1-H1C•••O5	2.912(6)	2.129	146.4
N2-H2A•••O8	2.940(5)	2.090	159.6
N2-H2B•••O12	2.904(5)	2.125	145.7
N2-H2C•••O10	2.922(4)	2.107	151.9
N3-H3A•••O15	2.790(5)	1.987	149.3
N3-H3B•••O19	3.040(5)	2.329	137.0
N3-H3C•••O17	2.924(4)	2.199	138.3
N4-H4A•••O22	2.853(5)	2.197	130.2
N4-H4B•••O26	3.113(4)	2.522	124.4
N4-H4C•••O24	2.861(5)	2.209	129.7

§Table S3. Distances and angles for C-H•••O interactions between crown ethers at 110 and 270 K.

contacted units	**list of atoms**	**C•••O distance** / Å	**H•••O distance** / Å	**C-H•••O angle** / °
110 K				
CE1•••CE1	[a]C19-H19B•••O4	3.631(3)	2.708	155.3
CE2•••CE2	[a] C35-H35B•••O8	3.534(2)	2.601	157.0
270 K				
CEA2•••CEA2	C47-H47B•••O8	3.480(5)	2.514	173.3
CEB2•••CEB2	C83-H83B•••O21	3.632(5)	2.676	168.8

[a] C-H•••O interactions in a complementary manner.

§Table S4. Distances and angles for C-H•••π interactions between crown ethers.

Temperature / K	contacted units	list of atoms	H•••C distance / Å	C•••C distance / Å	C-H•••C angle / °
110	**CE1•••CE1**	C46-H38B•••C38	2.753	3.461	128.90
130			2.754	3.465	129.14
150			2.759	3.471	129.30
170			2.767	3.480	129.38
190			2.772	3.487	129.54
210			2.786	3.497	129.86
230			2.799	3.507	129.70
250			2.815	3.520	129.48
270	**CEA1••• CEA1**		2.87	3.539	127
280			2.888	3.556	126.88
290			2.911	3.57	126.19
300			2.938	3.59	125.63
310			2.955	3.604	125.31
320			2.987	3.622	124.21

§Table S5. Distances and angles for C-H•••π interactions between crown ethers. The center of gravity of the phenylene ring of benzo[18]crown-6 is indicated as Pc.

Temperature / K	contacted units	list of atoms	H•••Pc distance / Å	C•••Pc distance / Å	C-H•••Pc angle / °
110	**CE1•••CE1**	Pc-H38B•••C38	3.015	3.941	156.34
130			3.022	3.950	156.48
150			3.031	3.959	156.36
170			3.043	3.970	156.45
190			3.054	3.982	156.58
210			3.074	3.993	156.62
230			3.089	4.006	156.36
250			3.108	4.023	155.90
270	**CEA1••• CEA1**		3.126	4.016	153.33
280			3.143	4.031	152.95
290			3.165	4.046	152.00
300			3.188	4.064	151.22
310			3.206	4.080	150.55
320			3.234	4.099	149.29

§Table S6. Distance between S•••S atoms less than the sum of the van der Waals radii of two S atoms between two [Ni(dmit)$_2$] anions at 110 and 270 K

contacted units	**list of atom**s	**S•••S distance** / Å
110 K		
D1•••D1	S3•••S5	3.7245(6)
D1•••D2	S2•••S6	3.5678(6)
	S2•••S11	3.4553(7)
	S4•••S11	3.3281(6)
	S4•••S13	3.3590(7)
D2•••D2	S8•••S15	3.8010(7)
D2•••D3	S12•••S16	3.5374(6)
	S14•••S16	3.4441(6)
D3•••D3	S18•••S20	3.7095(7)
270 K		
D1•••D2	S2•••S11	3.488(1)
	S2•••S16	3.511(1)
	S4•••S11	3.349(1)
	S4•••S13	3.435(1)
D1•••D4	S1•••S32	3.599(1)
	S6•••S32	3.576(1)
	S6•••S37	3.480(1)
	S8•••S37	3.428(1)
	S8•••S39	3.430(1)
D2•••D3	S12•••S26	3.426(1)
	S17•••S26	3.548(1)
	S17•••S28	3.451(1)
D3•••D3	S23•••S30	3.669(2)
D3•••D4	S22•••S36	3.527(1)
	S24•••S31	3.464(1)
	S27•••S36	3.563(1)
	S27•••S38	3.526(1)

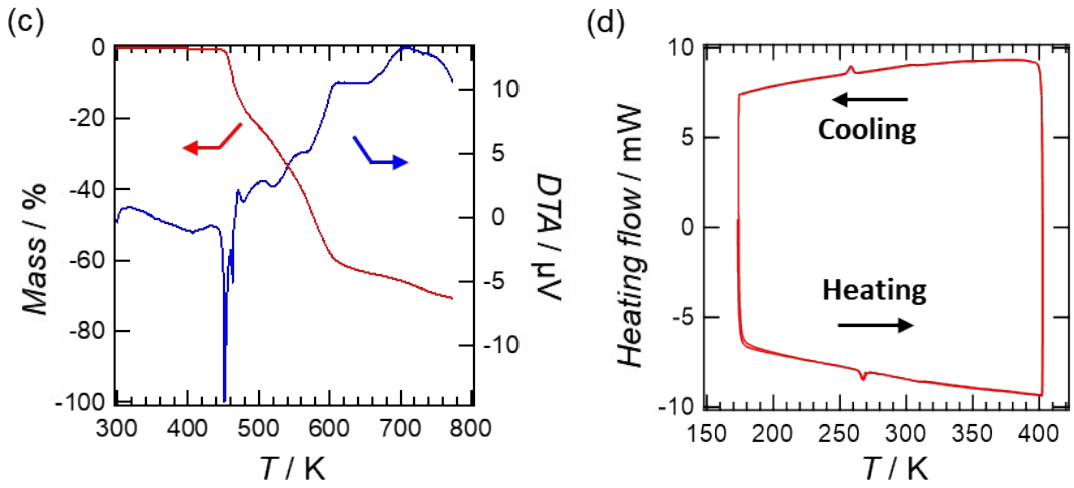

§Figure S2. (a) TG-DTA measurement for crystal **1**. (b) DSC from 170 to 400 K.

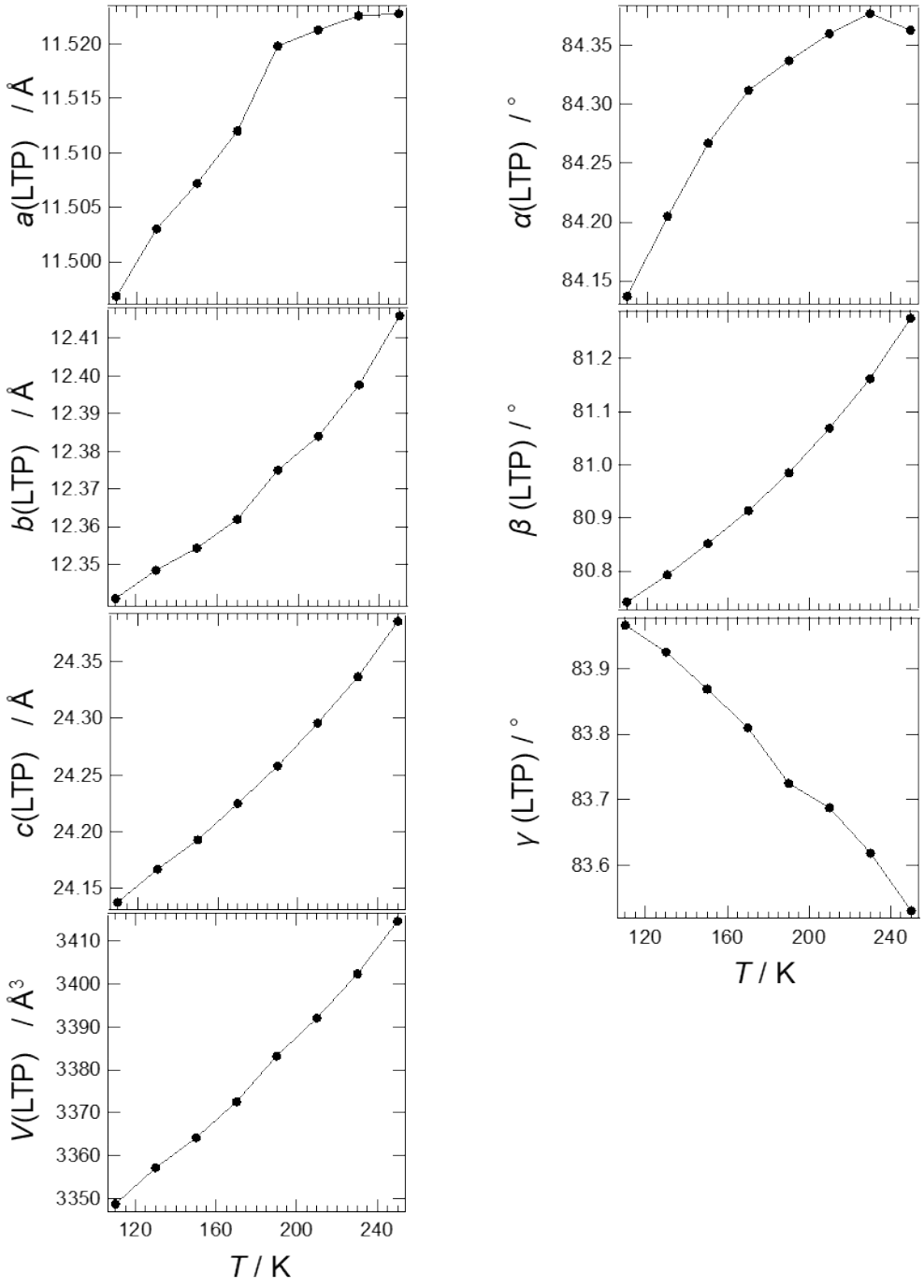

§Figure S3. Temperature dependence of unit cell dimensions and volume for crystal **1** over which the same crystal was studied. (LTP : Low Temperature phase)

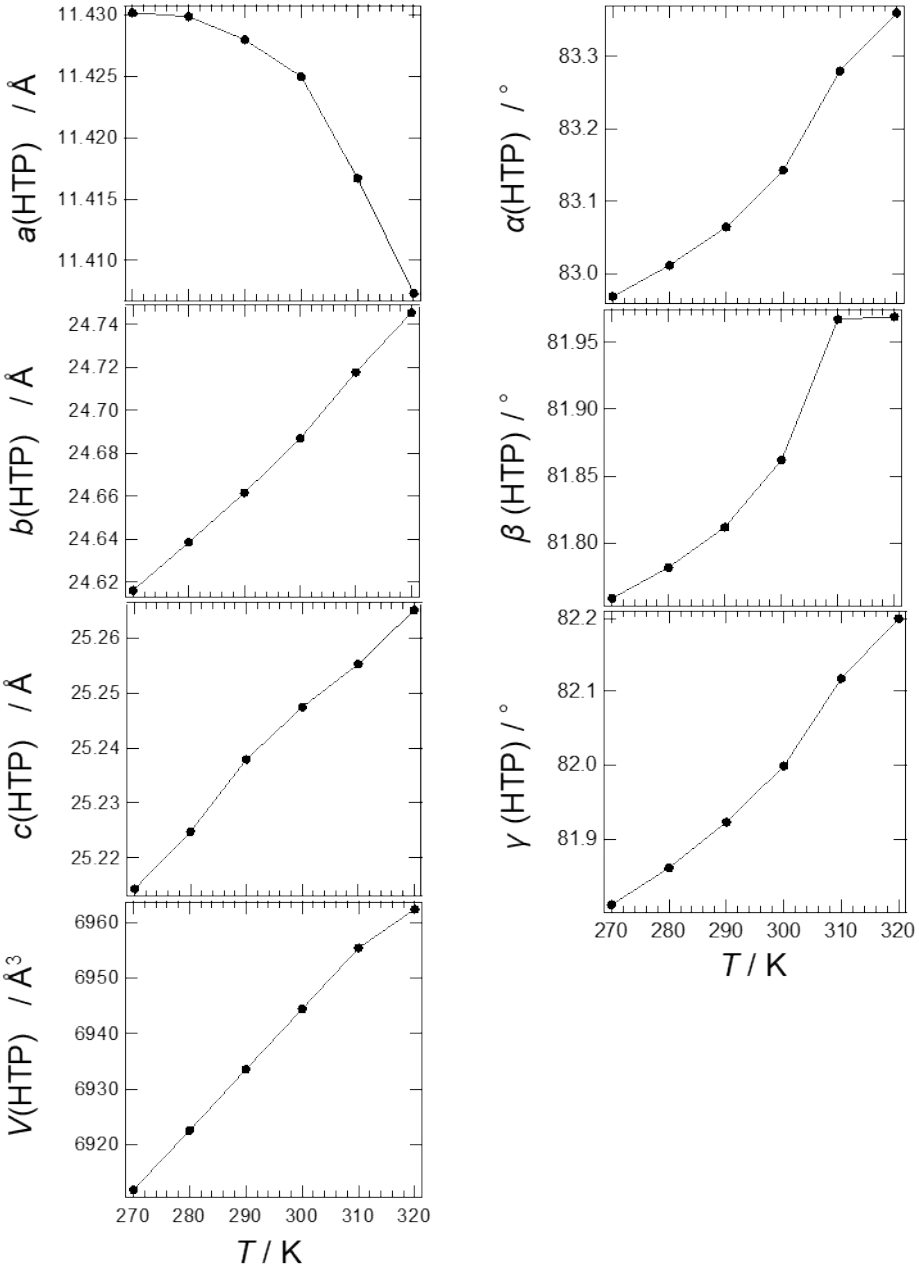

§Figure S4. Temperature dependence of unit cell dimensions and volume for crystal **1** over which the same crystal was studied. (HTP : High Themperature phase)

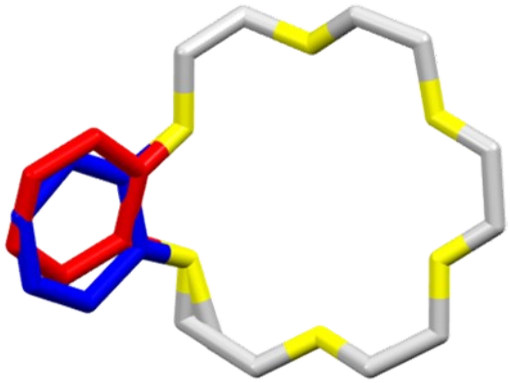

§Figure S5. Molecular structure **CEB2**, which is depicted in stick model, in crystal **1** at 310 K. The occupancies of the red and blue phenylene moieties in **CEB2** are 0.12, 0.88 and 0.29, 0.71 at 310 and 320 K, respectively.

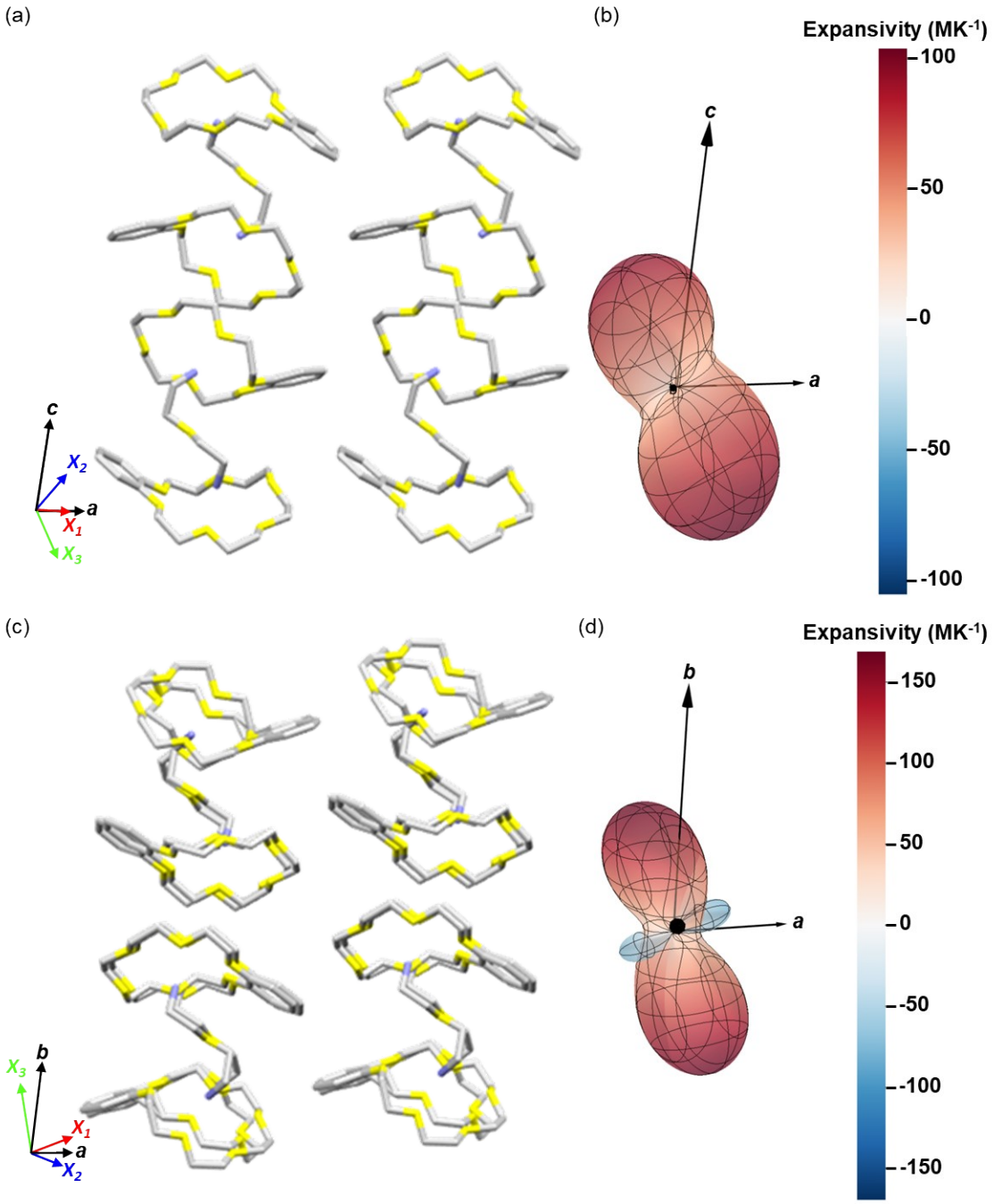

§Figure S6. The structure of supramolecular cations (a, c) and corresponding indicatrix plots (b, d) of LTP (a, b) and HTP (c, d) for **1**. PASCal indicatrix Plotter was used to plot the data. The software was obtained from the web site: https://www.pascalapp.co.uk/

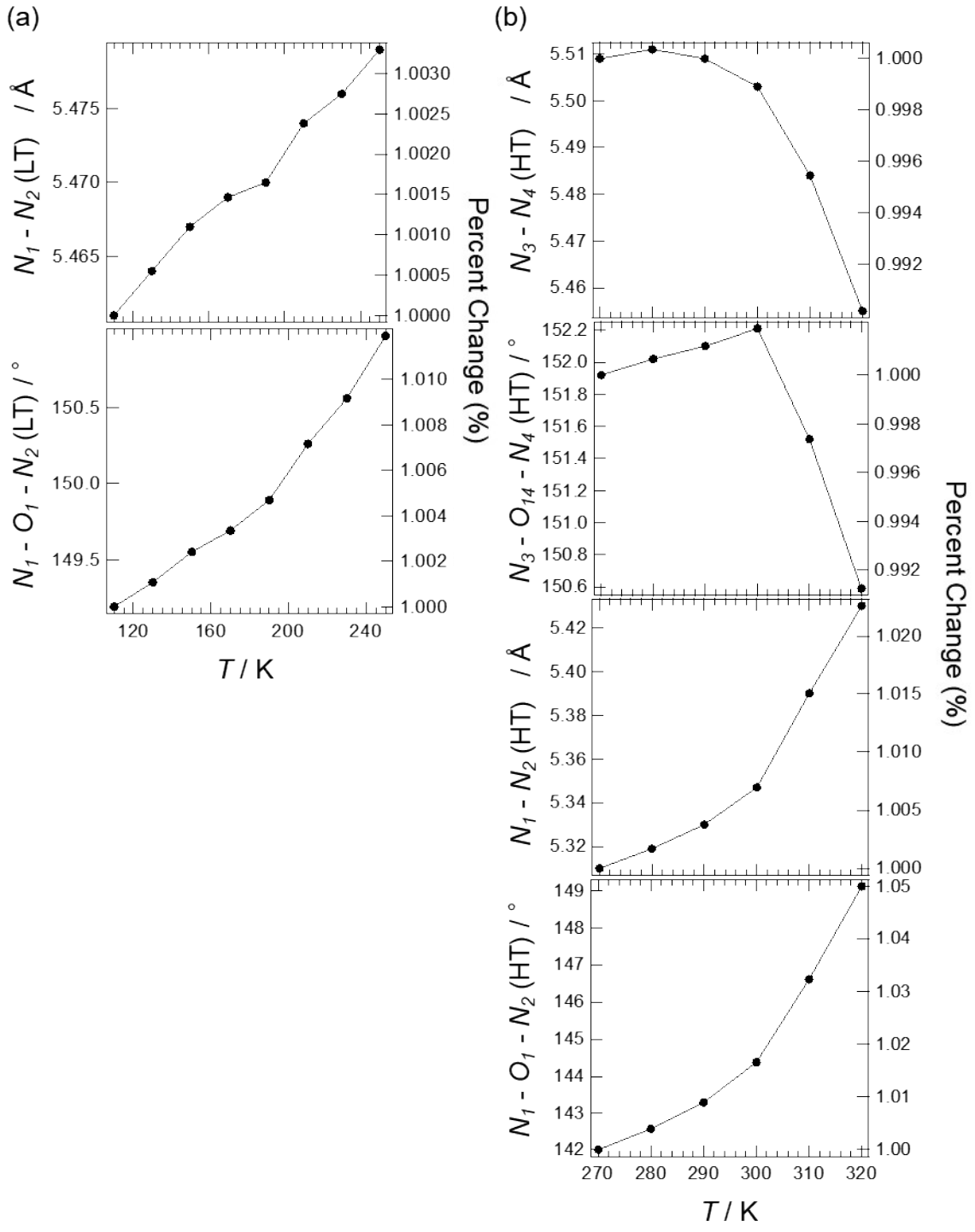

§Figure S7. Temperature dependence of the intramolecular N•••N interatomic distance and N•••O•••N angles (left axis) and compared with each value at 110 K (right axis) for crystal **1** LTP (a) and HTP (b).

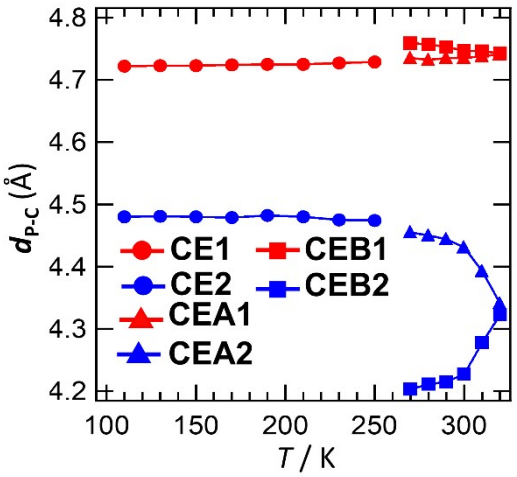

§Figure S8. Temperature dependence of $d_{P\text{-}C}$ in LTP and HTP.

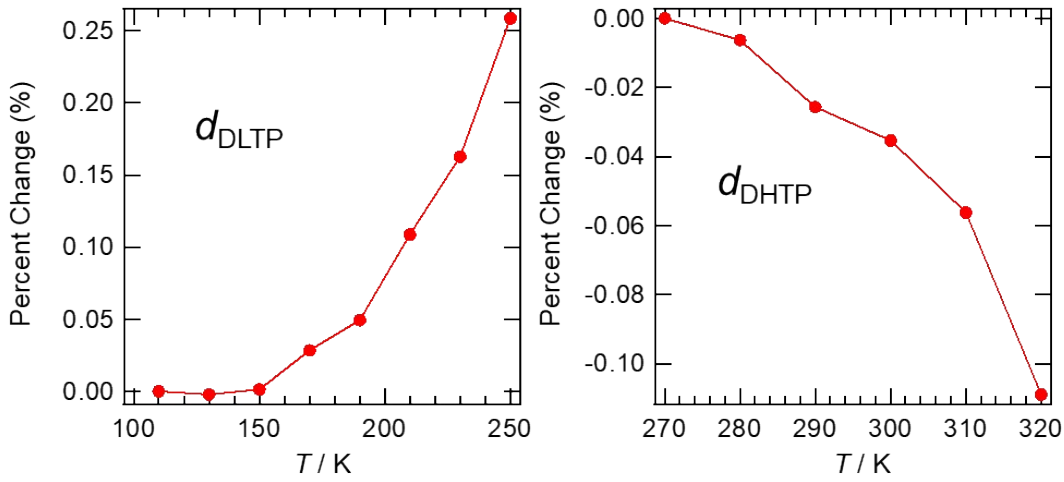

§Figure S9. Temperature dependence of percental change in the average net molecular length along the X_1 direction (denoted as (a) d_{DLTP} in LTP and (b) d_{DHTP} in HTP), resulting from the inclination between the (560) plane in LTP or the (1 -5 5) plane in HTP and the anion molecular plane.

In LTP and HTP, we defined the molecular plane for each $[Ni(dmit)_2]^-$ (LTP: D1~D3, HTP: D1~D4) molecule. Next, we calculated the angle θ between the molecular plane and the crystal plane [(560) or (1-55)] in each phase and determined $\cos\theta$ (the cosine value of the angle between the molecular plane and the X_1 or X_1' direction). For each molecule in LTP and HTP, we calculated the averaged value of $\cos\theta$, and based on the averaged value at the lowest temperature in each phase, we denoted the calculated temperature change rate as d_{DLTP} and d_{DHTP}.

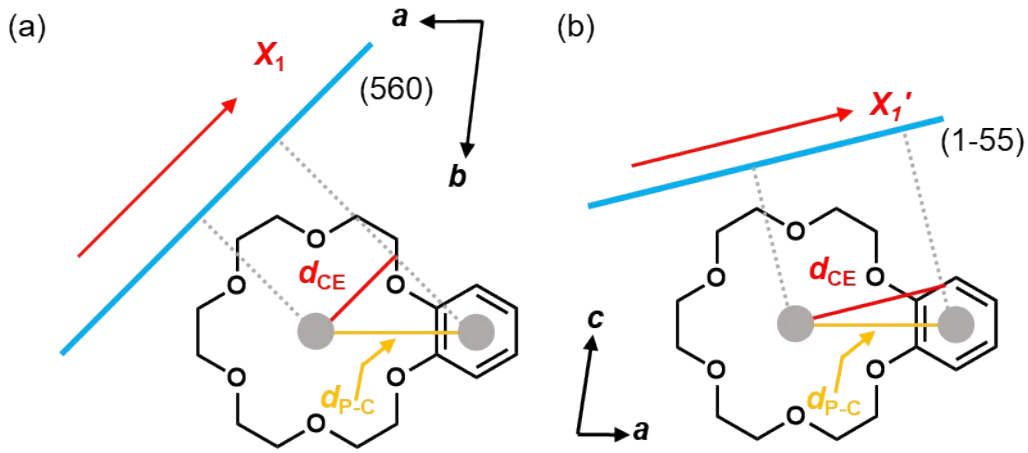

§Figure S10. Schematic views of **CE2** are shown for (a) LTP with the (560) plane viewed from the c axis and for (b) HTP with the (1-55) plane viewed from the b axis.

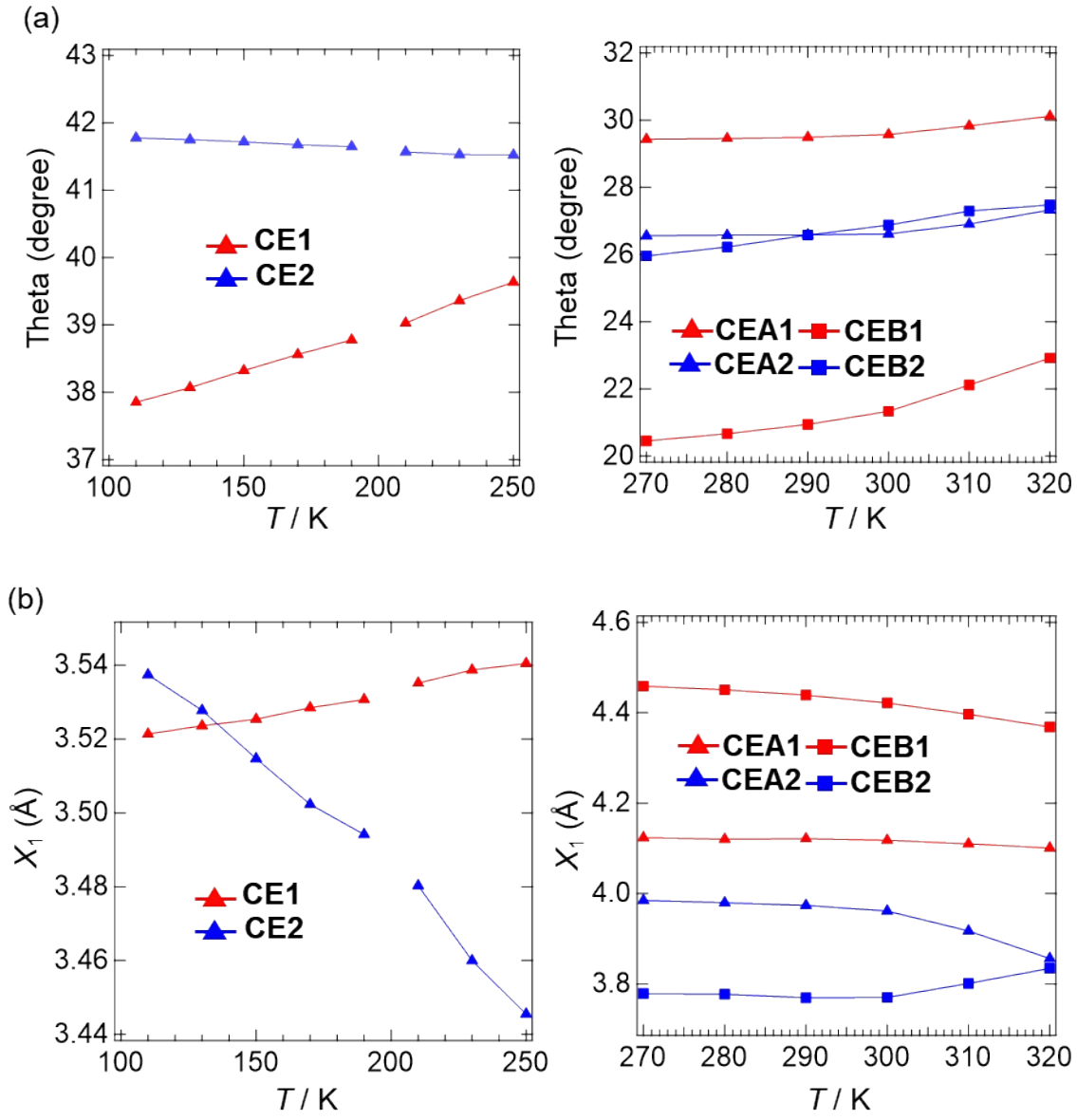

§Figure S11. Temperature dependence of (a) angle and (b) distance of d_{CE} measured in LTP and HTP

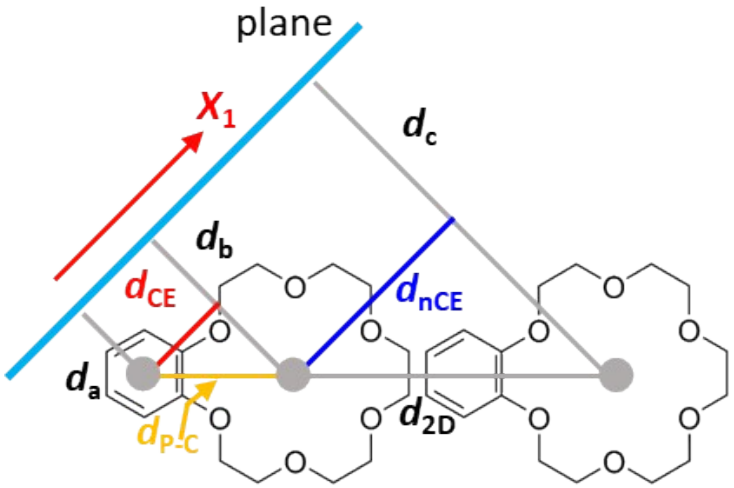

§Figure S12. Schematic view of the supramolecular cation layer and plane. The $d_{P\text{-}C}$ is the distance between the two centers of the crown ring of B[18]crown-6 and the phenylene ring. The d_{CE} and d_{nCE} are the projections of $d_{P\text{-}C}$ and *a*-axis length in the X_1 direction, respectively (see text). d_a is the distance from the center point of the phenylene group to the plane; d_b is the distance from the center point to the crown ether to the plane; dc is the distance from the center point to the plane of the adjacent crown ether; d_{2D} is the distance between the center point of the crown ether and the center point of the adjacent crown ether.

d_{CE} is obtained by the following equation.

$$d_{CE} = d_{P\text{-}C} \times cos\left\{\sin^{-1}\left[(d_b - d_a)/d_{P\text{-}C}\right]\right\}$$

d_{nCE} is obtained by the following equation.

$$d_{nCE} = d_{2D} \times cos\left\{\sin^{-1}\left[(d_c - d_b)/d_{2D}\right]\right\}$$

d_{CEave} calculated the center-to-center distance (d_{CE}) of each benzo[18]crown-6 molecule for all crown molecule pairs in the crystal and used the average value.

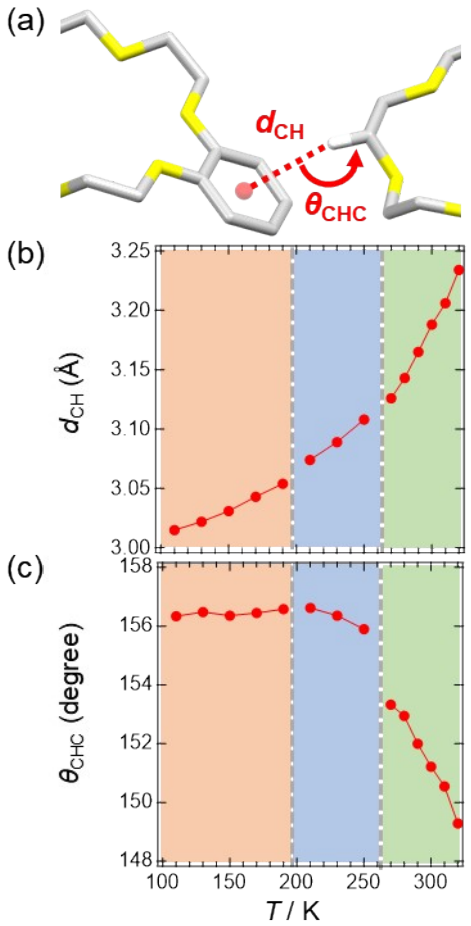

§Figure S13. (a) Schematic diagram of the nearest-neighbor distance (d_{CH}, red dotted line) between the carbon atom center of the phenylene group in B[18]Crown-6 and the hydrogen atom of the crown ether ring involved in the C-H•••π interaction, and the corresponding C-H•••C interatomic angle (θ_{CHC}, red arrow). (b) d_{CH} and (c) θ_{CHC} between **CE1•••CE1** (LTP) and **CEA1•••CEA1** (HTP).

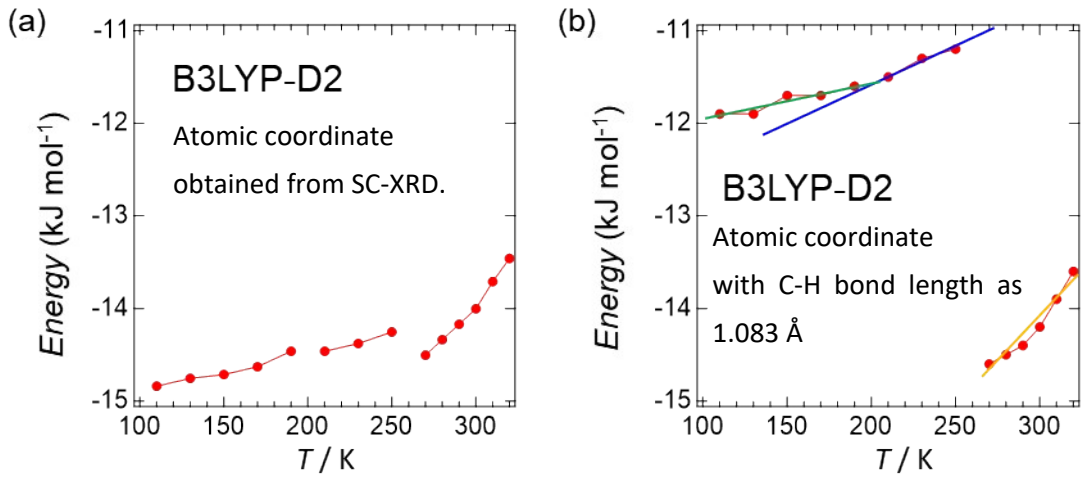

§Figure S14. Temperature dependence of interaction energies. (a) Interaction energies estimated from calculations at the B3LYP/6-31G(d,p) level using atomic coordinates obtained from X-ray crystal structure analysis. Grimme's D2 dispersion model was used for dispersion correction. Calculations were performed using the GAUSSIAN16 code package. (b) Interaction energies estimated from calculations at the B3LYP/6-31G(d,p) level with D2 dispersion correction, after correcting the C-H bond length to 1.083 Å, as obtained from neutron diffraction.

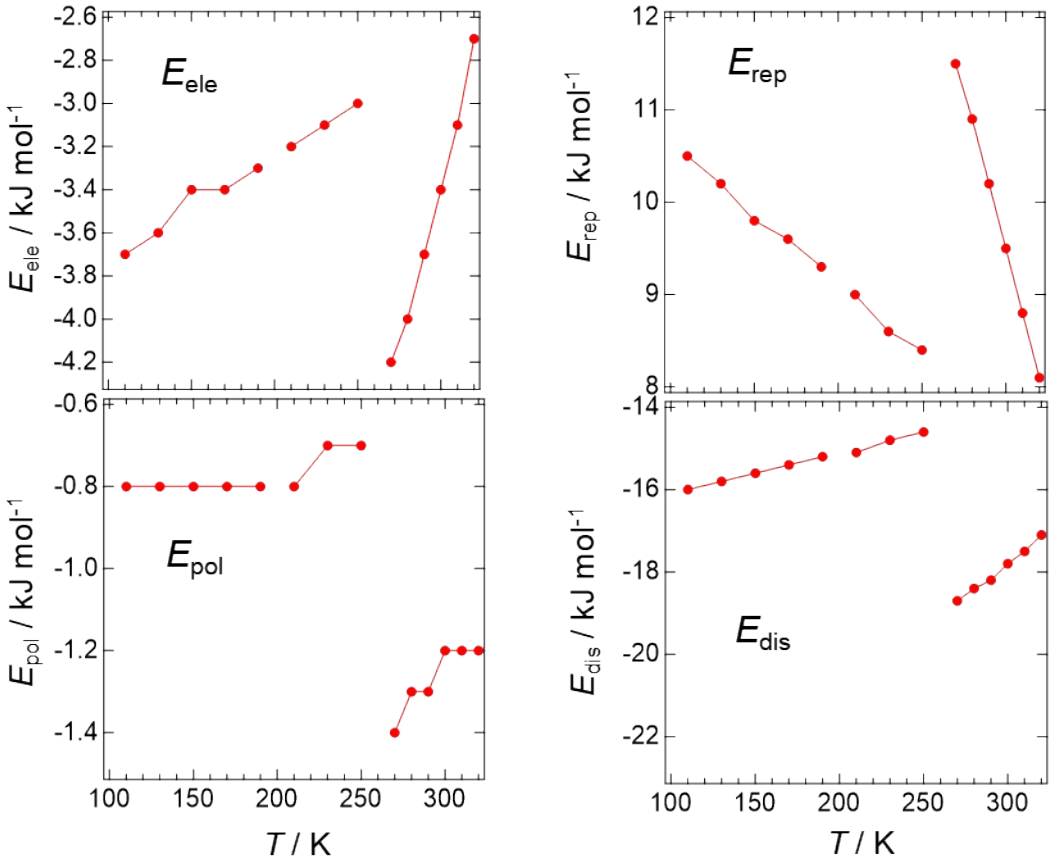

§Figure S15. Temperature-dependence of the four energy components of intermolecular interaction energies, electrostatic (E_{ele}), polarization (E_{pol}), exchange-repulsion (E_{rep}), and dispersion (E_{dis}) forces. These were isolated and quantified based on D2 dispersion correction after C-H bond length correction, using a combination of Crystal Explorer 21 and Gaussian 16 software.

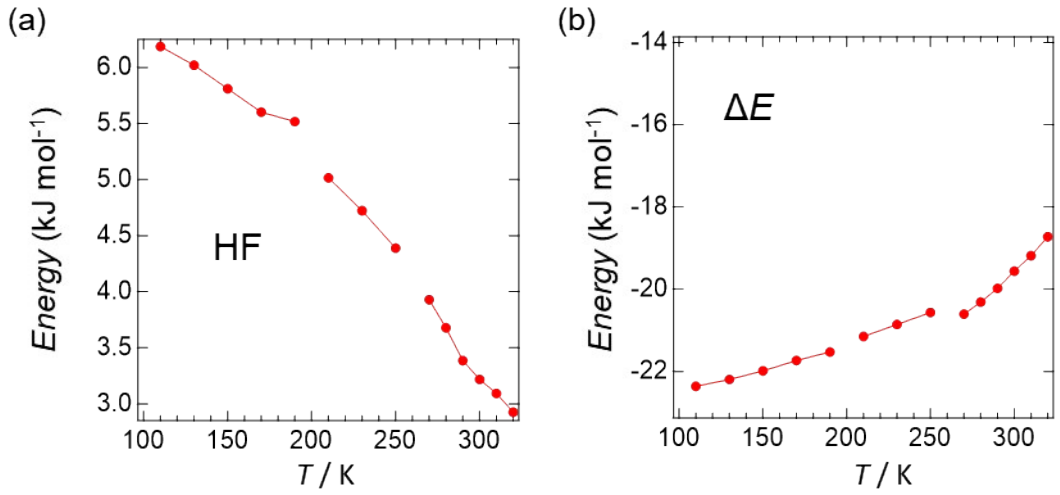

§Figure S16. (a) Interaction energies calculated at the HF/6-31G(d,p) level. Calculations were performed using the GAUSSIAN16. (b) Temperature dependence of the difference in interaction energies (*ΔE*) between the B3LYP-D3/6-31G(d,p) level (Figure 6c) and the HF/6-31G(d,p) level. *ΔE* corresponds to the dispersion force based on the D3 dispersion correction based on the atomic coordinate obtained from X-ray crystal structure analysis.

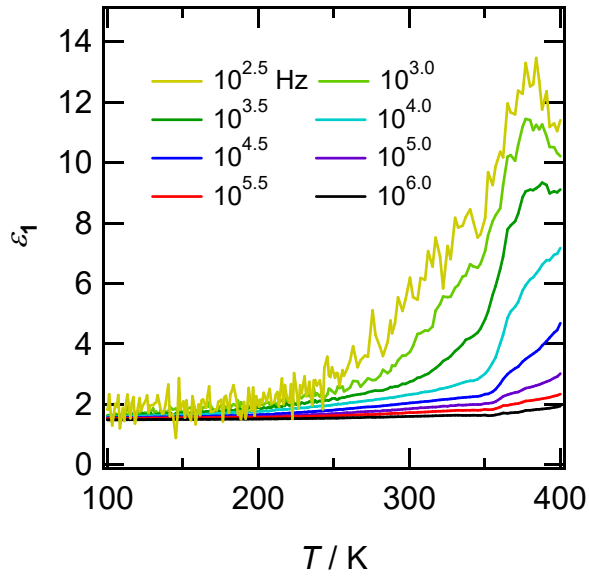

§Figure S17. Temperature- and frequency-dependent real part of dielectric permittivity from 100 to 400 K for pelletized sample of **1**.

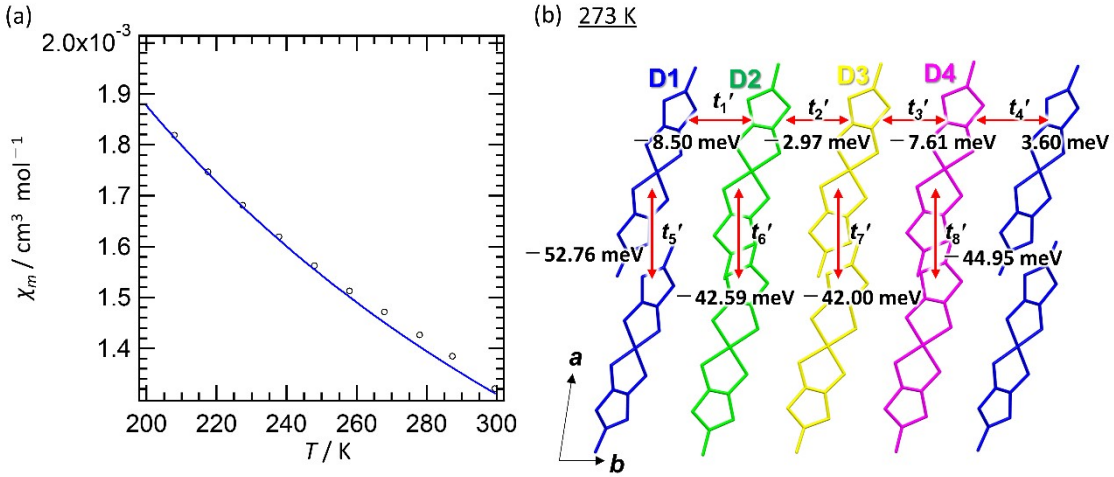

§Figure S18. (a) Temperature dependence of the molar magnetic susceptibility of crystal **1** (χ_m versus T plot). The blue lines are fitting curves reproduced using the 2D AF model with parameters Curie constant 0.43 cm^3 K mol^{-1}, magnetic exchange interaction J_1/k_B = 47.9 K, and J_2/k_B = 2.63 K. (b) Transfer integral between $[Ni(dmit)_2]^-$ for crystal **1** at 270 K.

§Table S7. Crystal data, data collection, and reduction parameters for crystal **1**.

Crystal	**1**		
Temperature / K	110	130	150
Crystal Dimensions / mm³	0.2×0.4×0.5		
Chemical formula	$C_{48}H_{62}N_2Ni_2O_{13}S_{20}$		
Formula weight	1633.61		
Crystal system	*Triclinic*		
Space group	$P\bar{1}$		
a / Å	11.4968(10)	11.5030(10)	11.5072(10)
b / Å	12.3410(10)	12.3485(10)	12.3544(10)
c / Å	24.1378(3)	24.1670(3)	24.1929(3)
α / deg	84.1370(10)	84.2050(10)	84.2670(10)
β / deg	80.7420(10)	80.7930(10)	80.8520(10)
γ / deg	83.9660(10)	83.9250(10)	83.8690(10)
V / Å³	3348.68(6)	3357.17(6)	3364.14(6)
Z	2		
D_{calc} / g·cm^{-3}	1.620	1.616	1.613
μ(Mo K_α) / mm^{-1}	1.244	1.241	1.238
$2\theta_{max}$ / deg	62.422	62.402	62.552
Reflections measured	89076	89410	89551
Independent reflections	18335	18389	18427
Reflections used	18335	18389	18427
R_1 [a]	0.0318	0.0324	0.0333
R_w (F^2) [a]	0.0740	0.0739	0.0742
GOF	1.034	1.029	1.032
CCDC No.	2444930	2444931	2444932

[a] $R_1 = \Sigma||F_o| - |F_c|| / \Sigma|F_o|$ and $R_w = (\Sigma\omega(|F_o| - |F_c|)^2 / \Sigma\omega F_o^2)^{1/2}$.

Crystal	**1**		
Temperature / K	170	190	210
Crystal Dimensions / mm³	0.2×0.4×0.4		
Chemical formula	$C_{48}H_{62}N_2Ni_2O_{13}S_{20}$		
Formula weight	1633.61		
Crystal system	*Triclinic*		
Space group	$P\bar{1}$		
a / Å	11.5120(10)	11.5198(10)	11.5213(10)
b / Å	12.3620(10)	12.3750(2)	12.3840(10)
c / Å	24.2250(3)	24.2580(4)	24.2959(3)
α / deg	84.3120(10)	84.3370(2)	84.3600(10)
β / deg	80.9140(10)	80.9850(10)	81.0690(10)
γ / deg	83.8100(10)	83.7250(10)	83.6880(10)
V / Å³	3372.54(6)	3383.25(9)	3392.09(6)
Z	2		
D_{calc} / g·cm^{-3}	1.609	1.604	1.599
μ(Mo K_α) / mm^{-1}	1.235	1.232	1.228
$2\theta_{max}$ / *deg*	62.030	62.608	61.650
Reflections measured	89704	89976	90228
Independent reflections	18464	18507	18568
Reflections used	18464	18507	18568
R_1 [a]	0.0340	0.0353	0.0362
R_w (F^2) [a]	0.0760	0.0774	0.0787
GOF	1.031	1.032	1.064
CCDC No.	2444933	2444934	2444938

[a] $R_1 = \Sigma||F_o| - |F_c|| / \Sigma|F_o|$ and $R_w = (\Sigma\omega(|F_o| - |F_c|)^2 / \Sigma\omega F_o^2)^{1/2}$.

Crystal	**1**		
Temperature / K	230	250	270
Crystal Dimensions / mm³	0.2×0.4×0.5		0.2×0.3×0.4
Chemical formula	$C_{48}H_{62}N_2Ni_2O_{13}S_{20}$		$C_{96}H_{124}N_4Ni_4O_{26}S_{40}$
Formula weight	1633.61		3267.22
Crystal system	*Triclinic*		
Space group	$P\bar{1}$		
a / Å	11.5226(10)	11.5228(2)	11.42954(10)
b / Å	12.3976(2)	12.4159(2)	24.6170(3)
c / Å	24.3366(3)	24.3855(3)	25.2122(2)
α / deg	84.3770(10)	84.3630(10)	82.9754(8)
β / deg	81.1620(10)	81.2760(10)	81.7651(8)
γ / deg	83.6190(10)	83.5310(10)	81.8090(8)
V / Å³	3402.38(8)	3414.70(9)	6911.28(12)
Z	2		
D_{calc} / g·cm^{-3}	1.595	1.589	1.570
μ(Mo K_α) / mm^{-1}	1.225	1.220	1.206
$2\theta_{max}$ / deg	61.436	59.850	58.670
Reflections measured	90563	90983	101119
Independent reflections	18634	18713	32371
Reflections used	18634	18713	32371
R_1 [a]	0.0382	0.0404	0.0547
R_w (F^2) [a]	0.0831	0.0879	0.1295
GOF	1.027	1.026	1.067
CCDC No.	2444936	2444937	2444935

[a] $R_1 = \Sigma||F_o| - |F_c|| / \Sigma|F_o|$ and $R_w = (\Sigma\omega(|F_o| - |F_c|)^2 / \Sigma\omega F_o^2)^{1/2}$.

Crystal	**1**		
Temperature / K	280	290	300
Crystal Dimensions / mm³	0.2×0.4×0.5		
Chemical formula	$C_{96}H_{124}N_4Ni_4O_{26}S_{40}$		
Formula weight	3267.22		
Crystal system	*Triclinic*		
Space group	$P\bar{1}$		
a / Å	11.4299(10)	11.4280(10)	11.4250(10)
b / Å	24.6386(3)	24.6616(3)	24.6870(3)
c / Å	25.2248(3)	25.2379(3)	25.2474(3)
α / deg	83.0120(10)	83.0650(10)	83.1430(10)
β / deg	81.7820(10)	81.8120(10)	81.8620(10)
γ / deg	81.8610(10)	81.9230(10)	81.9990(10)
V / Å³	6922.57(14)	6933.60(14)	6944.49(14)
Z	2		
D_{calc} / g·cm^{-3}	1.567	1.565	1.562
μ(Mo K_α) / mm^{-1}	1.204	1.202	1.200
$2\theta_{max}$ / deg	58.552	58.820	58.622
Reflections measured	101119	101196	101215
Independent reflections	32371	32410	32451
Reflections used	32371	32410	32451
R_1 [a]	0.0542	0.0597	0.0668
R_w (F^2) [a]	0.1279	0.1412	0.1553
GOF	1.062	1.066	1.080
CCDC No.	2444939	2444940	2444941

[a] $R_1 = \Sigma||F_o| - |F_c|| / \Sigma|F_o|$ and $R_w = (\Sigma\omega(|F_o| - |F_c|)^2 / \Sigma\omega F_o^2)^{1/2}$.

Crystal	**1**	
Temperature / K	310	320
Crystal Dimensions / mm³	0.2×0.4×0.5	
Chemical formula	$C_{96}H_{124}N_4Ni_4O_{26}S_{40}$	
Formula weight	3267.22	
Crystal system	*Triclinic*	
Space group	$P\bar{1}$	
a / Å	11.4167(2)	11.4073(16)
b / Å	24.7178(4)	24.7456(4)
c / Å	25.2552(3)	25.2650(4)
α / deg	83.2800(10)	83.3596(13)
β / deg	81.9670(10)	81.9689(12)
γ / deg	82.1170(10)	82.1983(13)
V / Å³	6955.42(19)	6962.43(18)
Z	2	
D_{calc} / g·cm^{-3}	1.560	1.558
μ(Mo K_α) / mm^{-1}	1.198	1.197
$2\theta_{max}$ / *deg*	58.558	58.398
Reflections measured	100676	100924
Independent reflections	32507	32541
Reflections used	32507	32541
R_1 [a]	0.0744	0.0856
R_w (F^2) [a]	0.1856	0.2228
GOF	1.009	1.047
CCDC No.	2444942	2444943

[a] $R_1 = \Sigma||F_o| - |F_c|| / \Sigma|F_o|$ and $R_w = (\Sigma\omega(|F_o| - |F_c|)^2 / \Sigma\omega F_o^2)^{1/2}$.

§Table S8. output file of *PASCal* calculation for crystal **1** between 110 to 250 K.

Output			Direction		
Axes	α (MK^{-1})	σα (MK^{-1})	*a*	*b*	*c*
X_1	−6.4187	2.1692	0.77	−0.6381	−0.0032
X_2	39.8465	4.1568	0.6006	0.7031	0.3808
X_3	105.0712	2.2411	0.6199	0.5858	−0.5221
V	139.1332	4.3935			

% Change in length						
T (K)	X_1 (%)	X_2 (%)	X_3 (%)	X_1,calc (%)	X_2,calc (%)	X_3,calc (%)
110	0	0	0	0.0269	−0.0562	−0.0268
130	0.0153	0.0431	0.1949	0.0141	0.0235	0.1834
150	0.0037	0.0753	0.3823	0.0013	0.1032	0.3935
170	−0.0014	0.1328	0.58	−0.0116	0.1829	0.6037
190	−0.0015	0.2337	0.7977	−0.0244	0.2626	0.8138
210	−0.01	0.304	0.9982	−0.0372	0.3423	1.024
230	−0.0444	0.4132	1.2287	−0.0501	0.4219	1.2341
250	−0.1055	0.5796	1.4882	−0.0629	0.5016	1.4442

Volume		
T / K	*V* / Å^3	*V*lin / Å^3
110	3348.682	3346.754
130	3357.17	3356.072
150	3364.141	3365.39
170	3372.536	3374.709
190	3383.247	3384.027
210	3392.084	3393.345
230	3402.379	3402.663
250	3414.703	3411.982

§Table S9. output file of *PASCal* calculation for crystal **1** between 270 to 320 K.

Output			Direction		
Axes	α (MK^{-1})	σα (MK^{-1})	*a*	*b*	*c*
X1	−75.5912	8.5752	0.9711	0.179	0.1576
X2	56.2074	4.1354	0.7988	−0.1392	−0.5853
X3	169.4957	7.0788	−0.5274	0.7832	−0.3293
V	149.7008	4.4276			

% change in length						
T (K)	X_1 (%)	X_2 (%)	X_3 (%)	X_1,calc (%)	X_2,calc (%)	X_3,calc (%)
270	0	0	0	0.0474	−0.0002	−0.0386
280	−0.0214	0.0497	0.126	−0.0282	0.056	0.1309
290	−0.0609	0.1095	0.2651	−0.1038	0.1122	0.3004
300	−0.1269	0.1696	0.4286	−0.1794	0.1684	0.4699
310	−0.2789	0.2546	0.655	−0.255	0.2246	0.6394
320	−0.3615	0.2585	0.8364	−0.3306	0.2808	0.8089

Volume		
T / K	*V* / Å^3	*V*lin / Å^3
270	6911.907	6912.537
280	6922.57	6922.884
290	6933.598	6933.231
300	6944.486	6943.579
310	6955.417	6953.926
320	6962.451	6964.273

Reference

50 G. Steimecke, H.-J. Sieler, R. Kirmse and E. Hoyer, *Phosphorus and Sulfur and the Related Elements*, 1979, **7**, 49–55.

51 G. M. Sheldrick, *Acta Cryst A*, 2015, **71**, 3–8.

52 O. V. Dolomanov, L. J. Bourhis, R. J. Gildea, J. a. K. Howard and H. Puschmann, *J Appl Cryst*, 2009, **42**, 339–341.

53 G. A. Bain and J. F. Berry, *J. Chem. Educ.*, 2008, **85**, 532.

54 W. J. Hehre, R. Ditchfield and J. A. Pople, *The Journal of Chemical Physics*, 1972, **56**, 2257–2261.

55 A. D. Becke, *The Journal of Chemical Physics*, 1993, **98**, 5648–5652.

56 S. F. Boys and F. and Bernardi, *Molecular Physics*, 1970, **19**, 553–566.

57 M. Xu, Y. Song, Y. Xu, Q. Sun, F. Long, N. Shi, Y. Qiao, C. Zhou, Y. Ren and J. Chen, *Chem. Mater.*, 2022, **34**, 9437–9445.

58 C. Yu, K. Lin, S. Jiang, Y. Cao, W. Li, Y. Wang, Y. Chen, K. An, L. You, K. Kato, Q. Li, J. Chen, J. Deng and X. Xing, *Nat Commun*, 2021, **12**, 4701.

59 S. Li, R. Huang, Y. Zhao, W. Wang, Y. Han and L. Li, *Advanced Functional Materials*, 2017, **27**, 1604195.

60 Y. Song, J. Chen, X. Liu, C. Wang, J. Zhang, H. Liu, H. Zhu, L. Hu, K. Lin, S. Zhang and X. Xing, *J. Am. Chem. Soc.*, 2018, **140**, 602–605.

61 P. Hu, J. Chen, J. Deng and X. Xing, *J. Am. Chem. Soc.*, 2010, **132**, 1925–1928.

62 Y. Sun, Y. Cao, S. Hu, M. Avdeev, C.-W. Wang, S. Khmelevskyi, Y. Ren, S. H. Lapidus, X. Chen, Q. Li, J. Deng, J. Miao, K. Lin, X. Kuang and X. Xing, *J. Am. Chem. Soc.*, 2023, **145**, 17096–17102.

63 W. Wang, R. Huang, W. Li, J. Tan, Y. Zhao, S. Li, C. Huang and L. Li, *Phys. Chem. Chem. Phys.*, 2014, **17**, 2352–2356.

64 M. Xia, F. Liang, X. Meng, Y. Wang and Z. Lin, *Inorg. Chem. Front.*, 2019, **6**, 2291–2295.

65 T. Matsuda, H. Tokoro, K. Hashimoto and S. Ohkoshi, *Dalton Trans.*, 2006, 5046–5050.

66 Z. Liu, K. Lin, Y. Ren, K. Kato, Y. Cao, J. Deng, J. Chen and X. Xing, *Chem. Commun.*, 2019, **55**, 4107–4110.